11th World Congress on Computational Mechanics (WCCM XI)
5th European Conference on Computational Mechanics (ECCM V)
6th European Conference on Computational Fluid Dynamics (ECFD VI)
E. Oñate, J. Oliver and A. Huerta (Eds)

FINITE ELEMENT ANALYSIS OF DAMPING MECHANISM OF AUTOCLAVED LIGHTWEIGHT AERATED CONCRETE PANELS FOR EXTERIOR WALLS OF STEEL STRUCTURES

MASAYUKI KOHIYAMA[1], MAKOTO OHSAKI[2], TOMOSHI MIYAMURA[3] AND TAKUZO YAMASHITA[4]

[1] Dept. of System Design Engineering, Keio University,
3-14-1 Hiyoshi, Kohoku-ku, Yokohama, 223-8522, Japan
E-mail: kohiyama@sd.keio.ac.jp

[2] Dept. of Architecture, Hiroshima University
1-4-1 Kagamiyama, Higashi-Hiroshima, 739-8527, Japan
E-mail: ohsaki@hiroshima-u.ac.jp

[3] Dept. of Computer Science, Nihon University
1 Nakagawara, Tokusada, Tamuramachi, Koriyama, 963-8642 Japan
E-mail: miyamura@cs.ce.nihon-u.ac.jp

[4] Hyogo Earthquake Engineering Research Center,
National Research Institute for Earth Science and Disaster Prevention (NIED)
1501-21 Nishikameya, Mitsuda, Shijimi-cho Miki, 673-0515, Japan
E-mail: tyamashi@bosai.go.jp

Key Words: *ALC Panel, Rocking Installation System, Plastic Deformation, Friction.*

1 INTRODUCTION

In designs of building structures, empirical damping models are usually used such as stiffness proportional damping and Rayleigh damping with a conventional damping factor, 0.02 or 0.03. However, a detailed analysis is expected to improve the damping models. In this study, the mechanical behavior of exterior walls made of autoclaved lightweight aerated concrete (ALC) is investigated using finite element analysis.

An ALC panel has beneficial features of lightness, heat and fire resistance, and pre-fabrication productivity. The ALC panels are often used for exterior wall cladding panels of middle-rise and high-rise buildings in Japan. 'Rocking installation system' is one of attaching methods of ALC panels, and it allows large story drift.

Matsuoka *et al.*[1] reported component tests of ALC external cladding panels adopting the rocking installation system, which were the same type of walls installed in a specimen of a full-scale 4-story steel moment frame building for three-dimensional shake-table tests[2–4]; the shake-table tests were conducted by Hyogo Earthquake Engineering Research Center (E-Defense), National Research Institute for Earth Science and Disaster Prevention (NIED), Japan. Both results of the component tests and the shake-table tests confirmed the safety of

the ALC external cladding panels under large story drift[4].

However, the influence of the ALC panels on the stiffness and damping characteristics should be clarified considering the detail of attachment. This study investigates these mechanisms using a parallel FE-analysis software, E-Simulator[5, 6], which is developed by E-Defense, NIED.

2 ANALYSIS MODEL OF ALC PANEL SPECIMEN

2.1 Geometry modeling

A numerical analysis model of the ALC panel specimen placed in the loading frame is constructed to reproduce the experiment reported by Matsuoka *et al.*[1]. Figure 1 shows a front elevation view of the model. In the experiment, six panels with a width of 600 mm, a height of 2,560 mm, and a thickness of 100 mm were used, whereas the model consists of two ALC panels to reduce the degrees of freedom (DOF).

The ALC panels, attachment plates, supporting members of steel angles and steel channels, and H-section steel girders of loading frame are modeled with 8-node hexahedral solid elements with linear displacement interpolation and incompatible modes. The section detail of the model is shown in Fig. 2. The ALC panels and all the steel plate members, such as attachment plates, channels, angles, webs, and flanges, are discretized into two layers of elements in the thickness direction. The columns and end parts of the upper girder of the loading frame is modeled with rigid beam elements, which are linked with pin joints, and both end surfaces of the upper girder are constrained by rigid beam elements to prevent stress concentration under an external load; the external load (forced displacement) is applied to the upper-right pin joint shown in Fig. 2.

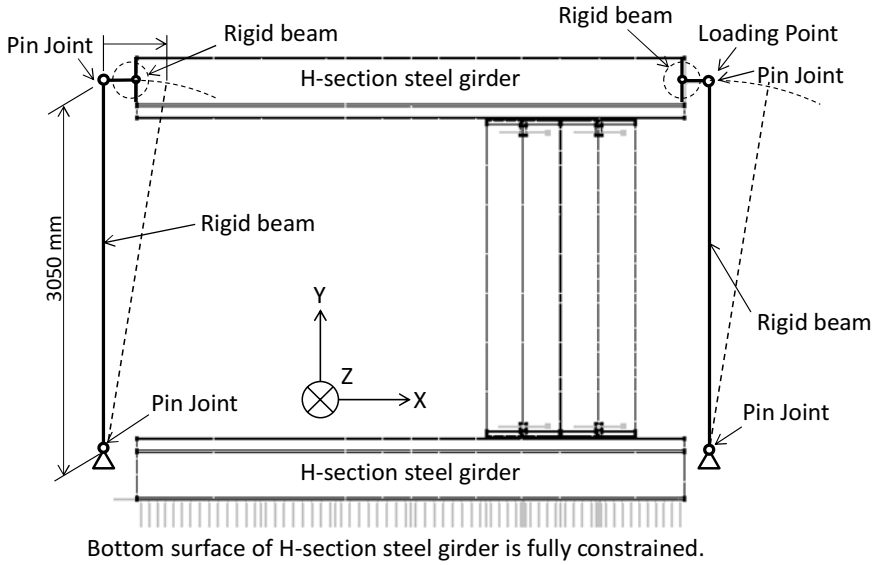

Figure 1: Numerical analysis model of ALC panel wall specimen and loading frame

An O-bolt is an attachment member inside an ALC panel. It connects with an anchor steel bar inside an ALC panel as shown in Fig. 3(a) and it also connects with an attachment plate as

shown in Fig. 2. It allows rotational displacement of an ALC panel around two horizontal axes and translational displacement in the direction of the member axis of the anchor steel bar. This mechanical condition is modeled with rigid beam elements and multi-point constraints as shown in Fig. 3(b).

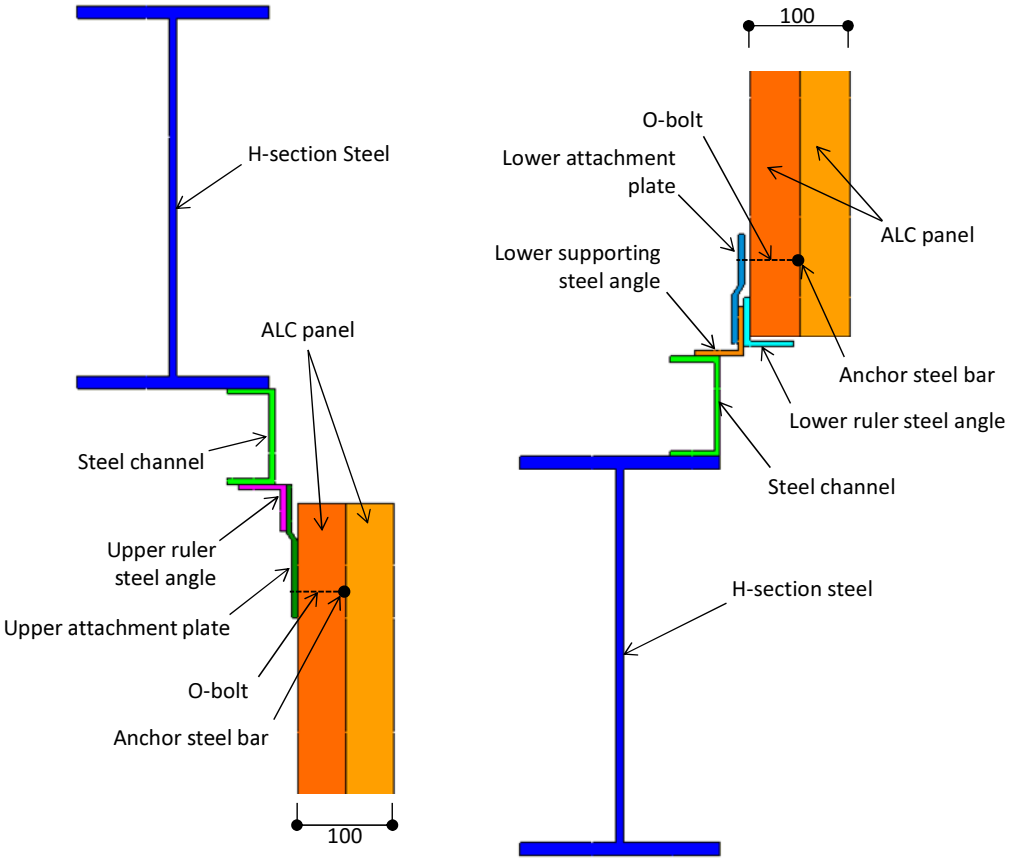

(a) Around upper attachment plate **(b)** Around lower attachment plate

Figure 2: Section detail of model

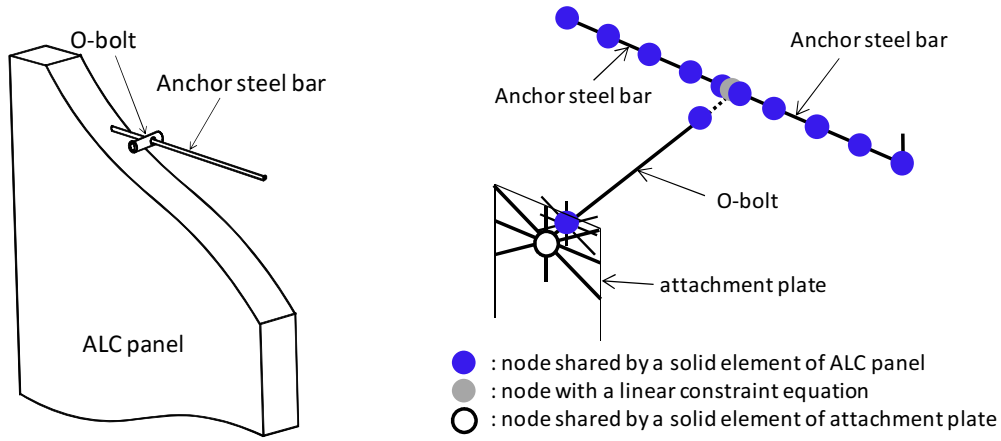

(a) Schematic view **(b)** Numerical analysis model

Figure 3: O-bolt and anchor steel bar inside ALC panel

An actual ALC panel contains not only anchor steel bar but also reinforcement steel bars. However, the reinforcement steel bars are neglected in the present model because the deformation of an ALC panel is considerably small in the analysis of this study. The model has 35,396 nodes, 22,972 hexahedral solid elements, and 66 rigid beam elements. The total number of DOFs is 106,188.

2.2 Material properties

The mass density, Young's modulus, and Poison's ratio of steel members of attachment plates, angles, channels, and H-section girders are 7.86×10^3 kg/m^3, 205.0 kN/mm^2, and 0.3, respectively. As a constitutive law, a bilinear model with isotropic hardening is used with the yield stress of 335 N/mm^2 and the hardening coefficient of 205.0 N/mm^2.

The density, Young's modulus, Poison's ratio, and compressive strength of the ALC panels are 6.50×10^2 kg/m^3, 2.47 kN/mm^2, 0.2, and 5.35 N/mm^2, respectively, which are evaluated using results of a sampling test for the product control. As a constitutive law, the extended hyperbolic Drucker-Prager model is employed to simulate the asymmetric behavior in tension and compression, and to prevent singularity at yielding in pure compression. The tensile and shear yield stresses are assigned to be 0.669 N/mm^2 and 0.717 N/mm^2, respectively, which are approximately an eighth of compressive strength. The hardening coefficient is 1/1000 of Young's modulus. The parameters for the extended Drucker-Prager model are determined from the yield stresses.

2.3 Contact conditions

Contact conditions are considered in the following three pairs of two faces: (i) adjoining lateral faces of two ALC panels, (ii) an attachment plate and its attaching face of an ALC panel, and (iii) the bottom surface of an ALC panel and a lower ruler steel angle. Detaching and reattaching processes are considered although the change of normal vectors on the faces is neglected.

Experimental data shows that the coefficient of friction (COF) between steel and concrete, ranges from 0.2 to 0.8[7, 8]. Because ALC is regarded to have smaller friction characteristics compared to those of ordinary concrete, the COF between a steel member and an ALC panel is assumed to be 0.1, a half of the minimum value of the experimental data range. Though the COF between ALC panels may be larger than that between steel and ALC, the same value, 0.1 is used in the analysis.

2.4 Loading conditions

Static alternately repeated cyclic loading with incremental deformation amplitude up to the drift angle of 1/50 (= 0.02) rad is conducted. Figure 4 shows loading program of horizontal forced displacement. In the analysis, forced displacement is applied to the upper-right pin joint shown in Fig. 2 as explained in Section 2.1, and the rotation angle of column is calculated by division of the forced displacement by 3,050 mm, which is the height of the column of the loading frame. Hereafter, the rotation angle of column is simply called deformation angle.

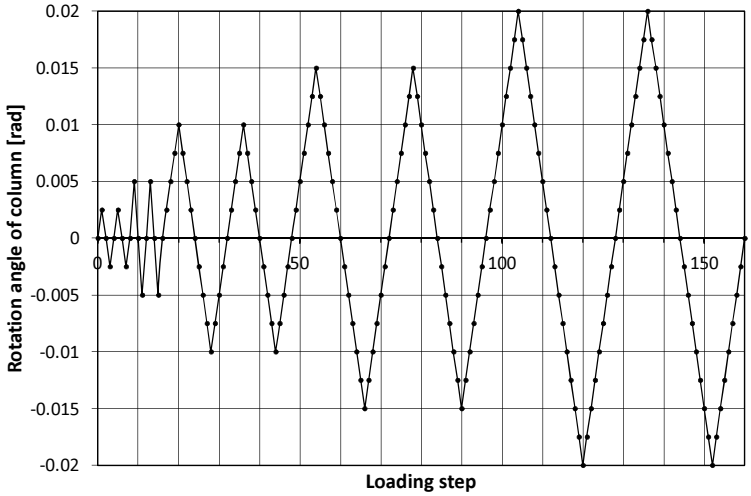

Figure 4: Loading program of horizontal forced displacement

3 ANALYSIS RESULT AND DISCUSSIONS

Figure 5(a) shows the lateral force–deformation angle relationship. The lateral resisting force drastically increased at a deformation angle of about 0.015 rad because corners of the ALC panels came into contact with the lower ruler steel angle. After this contact occurred, the slope of the curve in the unloading process became larger than that in the loading process. This difference was caused by the plastic deformation of ALC panels in the loading process; the enclosed area is proportional to the dissipated energy.

Figure 6 shows the distribution of equivalent plastic strain of elements of the ALC panel at a deformation angle of 0.02 rad; large plastic strain is observed in the ALC panel elements near the corner contacting the lower ruler steel angle and the elements around the upper O-bolt. After this plastic deformation, the lateral force magnitude at a small deformation angle became larger than zero. This is because a slide with friction between the two ALC panels occurred due to the residual deformation, which was caused by the contact between the ALC panels and the ruler steel angle.

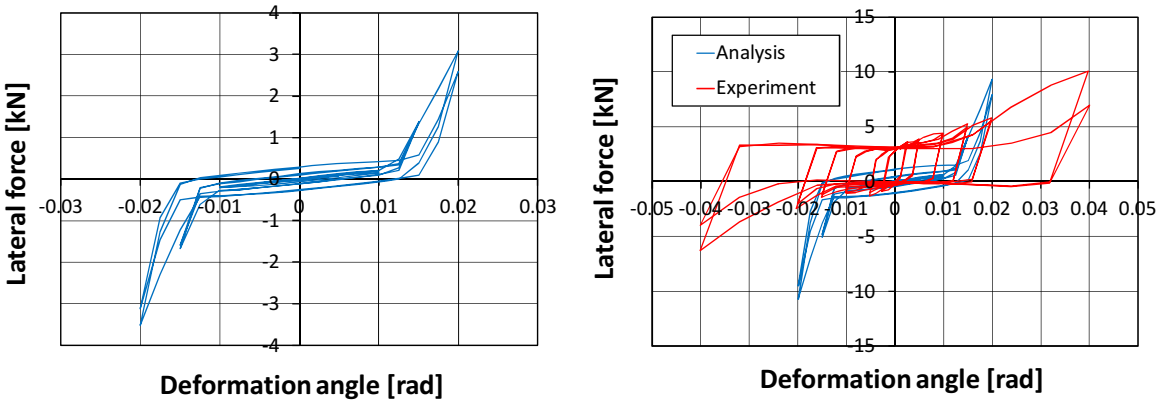

(a) Analysis result **(b)** Comparison with component test result[1]

Figure 5: Lateral force–deformation angle curves

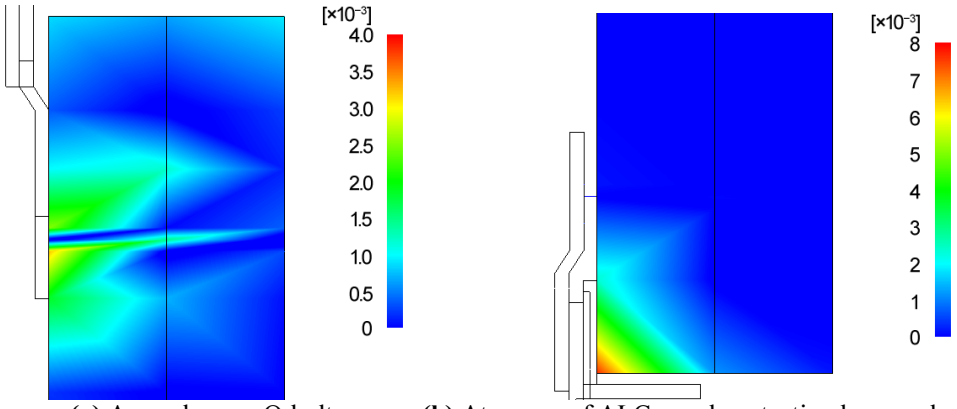

(a) Around upper O-bolt **(b)** At corner of ALC panel contacting lower ruler steel angle

Figure 6: Distribution of equivalent plastic strain of ALC panel elements at a deformation angle of 0.02 rad

Figure 5(b) shows the comparison of the lateral force–deformation angle relationship between the analysis and the experiment[1]. In the analysis, the lateral force equivalent to the six panel specimen was estimated as follows: resisting force generated by the friction between two ALC panels was multiplied by 5 and other resisting forces were multiplied by 3. The former resisting force was estimated by comparison of the analysis results of the following two cases: (i) only friction between ALC panels exists and (ii) no friction exists. In experimental data, lateral force of 3kN appears when the deformation angle increases in the positive direction. Matsuoka *et al.*[1] deduced that this was friction drag of loading apparatus, such as pin joints, because the force value was constant even in large deformation range. Other than this difference, it was observed that increase rates of the resisting force at a deformation angle of about 0.015 rad were rather gentle compared with the analysis result. The real specimen has looseness at a joint between an O-bolt and an attachment panel. However, this is not considered in the analysis model and consequently makes the difference.

Figures 7(a) and (b) show transitions of energy. Energy dissipation owing to the plastic deformation of the ALC panels and the friction became remarkably large when the deformation angle exceeds 0.015 rad because of the contact between corners of the ALC panel and the ruler steel angle.

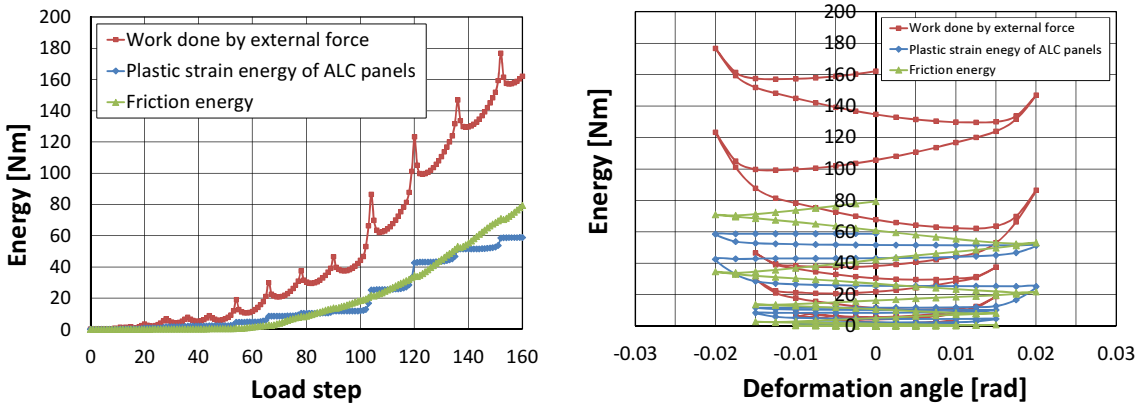

(a) Work done by external force and dissipated energy **(b)** Energy–deformation angle relationship

Figure 7: Transition of energy

The steep increases of the work done by the external force correspond to accumulation of elastic potential energy, but this has no relation to damping. Focusing on the cause of damping, plastic deformation and friction, the energy dissipated by the friction is comparable to the plastic strain energy of the ALC panels, and these energies are almost the same at the end of the loading steps in this analysis.

The analysis did not consider the joint looseness between an O-bolt and an attachment panel, and improved models and parameters can be introduced in a constitutive law of ALC and the COF for the frictional contact. However, it is suggested that the plastic deformation of ALC panels fulfill a significant role in damping mechanism of ALC external cladding panels when story drift is large.

4 CONCLUSIONS

Concluding remarks of the present study are summarized as follows:

- It was observed that energy dissipation owing to (i) the plastic deformation of the ALC panels and (ii) the friction between an ALC panel and a ruler steel angle became remarkably large when the deformation angle exceeded 0.015 rad because the corners of the ALC panel came into contact with the ruler steel angle.
- Under the condition that the looseness of a joint between an O-bolt and an attachment panel does not exist, the friction energy is almost comparable to the plastic strain energy of the ALC panels.

ACKNOWLEDGMENTS

This study is a part of Building Structures Working Group (Leader: Prof. Makoto Ohsaki, Hiroshima University) of E-Simulator Production Committee (Leader: Prof. Muneo Hori, The University of Tokyo) of NIED. The authors acknowledge the valuable contribution from the committee members, and the financial support by NIED. The contribution by Dr. Tomonobu Ohyama, Mr. Kiyoshi Yuyama, and Mr. Koji Nishimoto of Allied Engineering Corporation for model building and numerical analysis is also acknowledged. The authors would like to show sincere appreciation to Dr. Yuichi Matsuoka of Nippon Steel & Sumikin Engineering Co. Ltd., who has provided us with the experimental results.

REFERENCES

[1] Matsuoka, Y., Suita, K., Yamada, S., Shimada, Y., Akazawa, M., and Matsumiya, T. Evaluation of seismic performance of exterior cladding in full-scale 4-story building shaking table test. *J. Struct. Constr. Eng., Transaction of Architectural Institute of Japan* (2009) **74**:1353–1361, in Japanese.

[2] Yamada, S., Suita, K., Tada, M., Kasai, K., Matsuoka, Y., and Shimada, Y. Collapse experiment of 4-story steel moment frame: Part 1 outline of test results, *Proc. 14th World Conf. on Earthq. Eng.*, Beijing, China (2008) Paper ID: S17-01-004, 8 pages, DVD.

[3] Suita, K., Yamada, S., Tada, M., Kasai, K., Matsuoka, Y., and Shimada, Y. Collapse experiment of 4-story steel moment frame: Part 2 detail of collapse behavior, *Proc. 14th World Conf. on Earthq. Eng.*, Beijing, China (2008) Paper ID: S17-01-011, 8 pages, DVD.

[4] Matsuoka, Y. Suita, K., Yamada, S., and Shimada, Y. Non-structural component

performance in 4-story frame tested to collapse, *Proc. 14th World Conf. on Earthq. Eng.*, Beijing, China (2008) Paper ID: S17-01-014, 8 pages, DVD.

[5] Ohsaki, M., Miyamura, T., Kohiyama, M., Hori, M., Noguchi, H., Akiba, H., Kajiwara, K., and Ine, T. High-precision finite element analysis of elastoplastic dynamic responses of super-high-rise steel frames, *Earthq. Eng. Struct. Dyn.* (2009) **38**:635–654.

[6] Miyamura, T., Ohsaki, M., Kohiyama, M., Isobe, D., Onda, K., Akiba, H., Hori, M., Kajiwara, K., and Ine, T. Large-scale FE analysis of steel building frames using E-Simulator. *Progress of Nuclear Science and Technology* (2011) **2**:651–656.

[7] Matsuzawa, K., Ozawa, J., Watanabe, T. Experimental research on friction characteristics of steel and cementitious material, *Proc. Japan Concrete Institute* (2008) **30**:1141–1146, in Japanese.

[8] Katsuo, M., Ikenaga, M., Nagae, T., and Nakashima, M. Effect of velocity on dynamic coefficient of friction between steel and mortar, *Summaries of Technical Papers of Annual Meeting Architectural Institute of Japan.* (2008) **C-1**:639–640, in Japanese.